Electronic and structural properties of II-VI ternary alloys and superlattices

M.-H. Tsai
Department of Physics, University of Notre Dame, Notre Dame, Indiana 46556
and Department of Physics, National Sun Yat-Sen University, Kaohsiung 804, Taiwan

F. C. Peiris, S. Lee, and J. K. Furdyna
Department of Physics, University of Notre Dame, Notre Dame, Indiana 46556
(Received 13 March 2001; revised manuscript received 30 January 2002; published 24 May 2002)

Using a combination of first-principles molecular dynamics and conventional electronic-structure calculational methods, we examine the pronounced bowing phenomenon, which characterizes the direct energy gap E_g^Γ in $ZnSe_{1-x}Te_x$ alloys. The bowing of E_g^Γ is found to be attributable to significant electronegativity difference between the two anions. We also examine the structure of sinusoidally modulated $ZnSe_{1-x}Te_x$ superlattices whose composition varies in the range of $0.25<x<0.75$. We find an elongation of the Zn-Te bond and a contraction of the Zn-Se bond relative to those of the corresponding binary compounds. The elongation of the Zn-Te bond may explain the redshifts of E_g^Γ of 0.14 eV observed in the photoluminescence measurements on these supperlattices. We also study the electronic and structural properties of the $Zn_{1-x}Be_xSe$ and $Zn_{1-x}Cd_xSe$ alloys and find that in the $Zn_{1-x}Be_xSe$ alloys the Zn-Se bond length decreases slightly, while the Be-Se bond length increases by 10% relative to those of the binary compounds. This result suggests a softening of the Be-Se bond in the $Zn_{1-x}Be_xSe$ alloys. For $Zn_{1-x}Cd_xSe$, the Zn-Se and Cd-Se bond lengths deviate from those of the respective binary compounds by not more than 2%. We also find that the direct band gap E_g^Γ as a function of x bows down for both $Zn_{1-x}Be_xSe$ and $Zn_{1-x}Cd_xSe$ in agreement with experimental data.

DOI: 10.1103/PhysRevB.65.235202 PACS number(s): 71.22+i

I. INTRODUCTION

The ternary alloy $ZnSe_{1-x}Te_x$ is known to exhibit a strikingly nonlinear dependence of the direct energy gap E_g^Γ on the composition x. Specifically, the value of E_g^Γ as a function of x exhibits a relatively deep minimum of 2.22 eV at $x=0.65$,[1] significantly lower than E_g^Γ of either of the binary end points (2.702 for $x=0.0$ and 2.44 for $x=1.0$). The value of the bowing coefficient for this material (i.e., the parameter which determines the nonlinearity of the energy gap $E_g^\Gamma(x)$ is 1.621—among the largest ever reported for a ternary system. Furthermore, recently Yang *et al.*[2] and Lee *et al.*[3] performed photoluminescence (PL) measurements on short-period sinusoidally modulated $ZnSe_{1-x}Te_x$ superlattices grown by molecular beam epitaxy (MBE) with x varying between 0.25 and 0.75 (i.e., with an average x of 0.50) and a periodicity ranging between 13.5 and 58 Å, and found redshifts of E_g^Γ down to 2.08 eV, which is even lower (by as much as 0.14 eV) than the lowest E_g^Γ value of the alloy. These unusual electronic properties of the $ZnSe_{1-x}Te_x$ system are still not well understood.

In semiconductor ternary alloys the cation-anion bond lengths are usually very nearly conserved, i.e., over the entire composition range of the alloy they retain nearly the same values as the cation-anion bond lengths, which exist in the ''parent'' binary compounds. Whether this property is universally true for semiconductor ternary alloys is an interesting question. Intuitively, one may expect that it may become increasingly difficult to conserve the cation-anion bond lengths when the difference between the sizes (i.e., the covalent radii) of the anions and the cations becomes excessive. For the II-VI ternary alloy $Zn_{1-x}Be_xSe$ the Be ion (with a covalent radius of 0.90 Å) is much smaller than the Zn ion (whose covalent radius is 1.25 Å).[4] Due to this large discrepancy between the covalent radii in the $Zn_{1-x}Be_xSe$ alloy system, it is relevant to question whether the Zn-Se and Be-Se bond lengths remain unchanged in this alloy. Since the electronic structure strongly depends on the cation-anion bond lengths in the alloy, the deviation in the bond lengths in this alloy may in turn have significant influence on its electronic structure and related physical properties. Recently, the direct band gaps E_g^Γ's in the $Zn_{1-x}Be_xSe$ family of alloys were measured by Peiris *et al.* for x up to about 0.35.[5] The measured E_g^Γ as a function of x in this region is approximately linear with a possible slight downward bowing. More recently, Chauvet, Tournie, and Faurie measured E_g^Γ of the $Zn_{1-x}Be_xSe$ alloy in the whole composition range.[6] They fitted the variation of E_g^Γ into the quadratic equation $E_g^\Gamma(x)=2.80(1-x)+5.60x-0.97x(1-x)$, which showed significant bowing of E_g^Γ. Peiris *et al.* also measured E_g^Γ's for the $Zn_{1-x}Cd_xSe$ alloys and found that E_g^Γ bows down slightly.[4]

To understand the electronic and structural properties of these II-VI ternary alloys and superlattices mentioned above we carry out the present study, in which we employ a combination of first-principles molecular-dynamics (MD)[7–9] and conventional electronic-structure calculation methods.[10] The MD method is used in the energy minimization application, which provides an efficient means to obtain equilibrium atomic positions. This in turn enables us to calculate the electronic structure, which strongly depends on the atomic arrangement.

II. CALCULATION METHODS

The MD method used in this study originates from the Sankey-Niklewski *ab initio* multicenter MD method,[7] later

modified to include charge transfer.[8] Most recently, this procedure has been extended to enable self-consistent calculation of the full charge densities and the corresponding potentials.[9] This method uses norm-conserving pseudopotentials[11,12] with the Ceperley-Alder exchange-correlation potentials.[13] The basis set is composed of Bloch sums of s, p_x, p_y, and p_z pseudoatom orbitals. To accurately treat charge densities and potentials in interstitial regions, as well as their nonspherical parts inside the atoms, we use plane-wave expansions and the fast-Fourier-transform technique for obtaining the matrix elements. This method has worked well for semiconductors.[14–19]

The conventional electronic-structure calculation method is the pseudofunction (PSF) method,[10] which uses the linear theory of Andersen[20] for solving the Schrödinger equations inside the muffin-tin spheres similar to the well-known linear augmented plane wave (LAPW) and linear muffin-tin orbital (LMTO) methods.[20] The basis set used in the PSF method contains two sets of Bloch sums of muffin-tin orbitals. One uses exponentially decaying tailing functions described by the spherical Hankel functions, which are suitable for describing localized states. The other contains oscillating tailing functions described by the spherical Neumann functions, which are suitable for describing extended itinerant states. The pseudofunctions are smooth mathematical functions expandable by a minimal set of plane waves. They are simply devised to efficiently calculate, by means of the fast-Fourier-transform technique, the interstitial and nonspherical parts of the charge density and potential. The choice of the number of plane waves is guided by the criterion $G_{\max}R_{\mathrm{MT}}>n$, here $n=7$, 5, and 3 for d, p, and s orbitals, respectively, and $G_{\max}$ and R_{MT} are the magnitudes of the cutoff reciprocal vector and the smallest muffin-tin radius, respectively. The PSF method uses the Hedin-Lundqvist[21] form of local density approximation (LDA) for the exchange-correlation potential.

TABLE I. Bond lengths $d_{\text{Zn-Se}}$ and $d_{\text{Be-Se}}$, in Å in the $Zn_{1-x}Be_xSe$ alloy.

x	$d_{\text{Zn-Se}}$	$d_{\text{Be-Se}}$
0.00	2.480	
0.25	2.475	2.364
0.50	2.471	2.366
0.75	2.425	2.317
1.00		2.146

LDA is well known to underestimate the band gaps of semiconductors. This deficiency can be improved by the quasiparticle or density-gradient correction. It has been shown the correction is insensitive to the **k** point.[22] Thus, the LDA still predicts reliable conduction band with approximately a rigid shift from the experimental E_g^{Γ} data.

The semiconductor ternary alloys are random alloys. The cations and anions should be treated statistically for the $A_{1-x}B_xC$- and $AB_{1-x}C_x$-type alloys, respectively. Due to the limitation of our calculation methods, we cannot use virtual-crystal-type calculations to take into account statistics. Thus we have to use ordered-crystal models. Here, we would like to caution the readers that the use of ordered-crystal models might result in structural properties that are different from real alloy samples. In the calculation of the structural properties, we have started our MD calculations with the zinc blende structure and let the calculated forces to move the atoms to their equilibrium positions. We have chosen the basic cubic cell as the unit cell. In the unit cell there are four C anions and three A and one B, two A and two B, and one A and three B cations, respectively, for $x=0.25$, 0.50, and 0.75 for the $A_{1-x}B_xC$-type alloys. For the $AB_{1-x}C_x$-type alloy we use similar structural models. Dur-

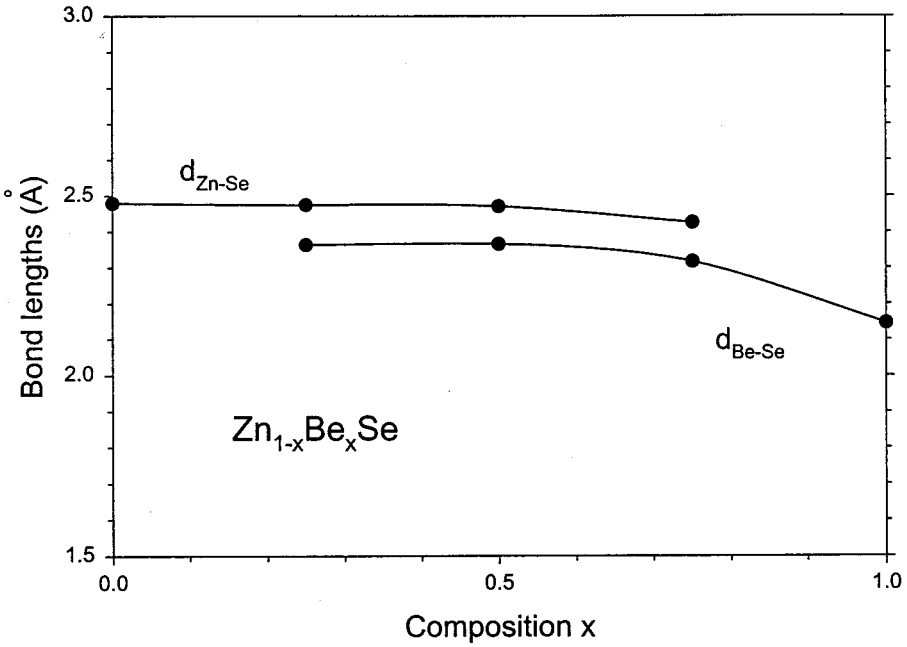

FIG. 1. Bond lengths $d_{\text{Zn-Se}}$ and $d_{\text{Be-Se}}$ are plotted with respect to the composition x for the $Zn_{1-x}Be_xSe$ alloy.

TABLE II. The coordinates of the atoms in the cubic unit cell for $x=0.25$. The values are given in terms of the equilibrium lattice constant $\eta=0.00845$.

Atoms	x	y	z
Zn	0.25	0.25	0.25
Zn	0.25	0.75	0.75
Zn	0.75	0.25	0.75
Be	0.75	0.75	0.25
Se	$-\eta$	$-\eta$	η
Se	$-\eta$	$0.5+\eta$	$0.5-\eta$
Se	$0.5+\eta$	$-\eta$	$0.5-\eta$
Se	$0.5+\eta$	$0.5+\eta$	η

TABLE III. The coordinates of the atoms in the cubic unit cell for $x=0.50$. The values are given in terms of the equilibrium lattice constant $\eta=0.01629$.

Atoms	x	y	z
Zn	0.25	0.25	0.25
Zn	0.25	0.75	0.75
Zn	0.75	0.25	0.75
Be	0.75	0.75	0.25
Se	0.0	$-\eta$	0.0
Se	0.0	$0.5+\eta$	0.5
Se	0.5	$-\eta$	0.5
Se	0.5	$0.5+\eta$	0.0

ing the MD calculations, we did not impose any constraint or any symmetry on the movement of the atoms other than the periodicity of the unit cell.

III. LATTICE CONSTANTS AND BOND LENGTHS

We first use the MD method in the energy minimization application to obtain the lattice constants of the binaries ZnSe, ZnTe, BeSe, and CdSe. Using the basic cubic unit cell and sampling the Γ point, we obtain the lattice parameters of 5.728, 5.945, 4.955, and 6.045 Å, respectively, for these four materials. These values differ from the corresponding experimental values of 5.6676, 6.101, 5.139, and 6.05 Å (Ref. 23) by $+1.1$, -2.6, -3.6, and -0.1%, respectively. The MD method is also used to calculate the equilibrium lattice constants and the Zn-Se and Be-Se bond lengths $d_{\text{Zn-Se}}$ and $d_{\text{Be-Se}}$, of the $Zn_{1-x}Be_xSe$ alloy for $x=0.25$, 0.50, and 0.75. For each x value, we have varied the lattice constant. For each lattice constant we have obtained equilibrium atomic positions using the criterion that the force acting on each atom is less than 0.1 eV/Å. The bond lengths are calculated from the equilibrium atomic positions for the lattice constant with the minimum total energy. The calculated equilibrium lattice constants are 5.650, 5.581, and 5.410 Å for $x=0.25$, 0.50, and 0.75, respectively. At $x=0.50$, the equilibrium lattice constant differs from that determined by the Vegard's rule 5.342 Å by 4.5%. The calculated $d_{\text{Zn-Se}}$ and $d_{\text{Be-Se}}$ are tabulated in Table I and are plotted in Fig. 1. The calculated coordinates of the atoms in the cubic unit cell given in terms of the equilibrium lattice constant are tabulated in Tables II, III, and IV for $x=0.25$, 0.50, and 0.75, respectively. By ignoring some negligible deviations these coordinates can be described by a single parameter η that characterizes the deviation from the atomic positions of the zinc blende structure. Tables II, III, and IV show that the Zn and Be cations remain at the fcc sublattice. Only the common anions, i.e., Se ions, adjust their positions to accommodate the size difference of the Zn and Be cations. Our results show that $d_{\text{Zn-Se}}$ deviates from that of the Zn-Se binary by not more than about 2%, while $d_{\text{Be-Se}}$ increases significantly from that of the Be-Se binary by as much as 10%. However, it is interesting to note that $d_{\text{Be-Se}}$'s are approximately elongated with the same extent for $x=0.25$, 0.50, and 0.75. This result suggests that the Be-Se bond in the $Zn_{1-x}Be_xSe$ alloys be significantly softened. The physical reason of this behavior might be that the Be atom has a smaller electronegativity (being 1.57 vs 1.65 of the Zn atom[4]), so that the Be-Se bond is more ionic and less rigid than the Zn-Se bond. This argument is consistent with the results of our electronic-structure calculations to be stated later. We find that the charges inside the Be muffin-tin spheres in the alloys are significantly smaller than that in the Be-Se binary. This trend is opposite for the charges in the Zn muffin-tin spheres. Thus, there is a charge transfer from the Be ions to the Zn ions in the $Zn_{1-x}Be_xSe$ alloys. The near conservation of the Zn-Se bond length and the significant increase of the equilibrium lattice constant (4.5% at $x=0.50$), which tends to approach that of the Zn-Se binary, indicate that the Zn-Se bond not only tends to conserve the bond length but also the bond angles. This tendency of the Zn-Se bond to conserve both bond length and angles reflects that the Zn-Se bond is more covalent than the Be-Se bond.

We have also studied the $Zn_{1-x}Cd_xSe$ alloy—which involves cations of comparable covalent radii—in order to see whether the cation-anion bond lengths are conserved when the sizes of the constituent cations do not differ greatly. By a similar procedure we calculate the lattice constant and then the Zn-Se and Cd-Se bond lengths in the $Zn_{1-x}Cd_xSe$ alloys. The calculated equilibrium lattice constants are 5.807, 5.877, and 5.946 Å for $x=0.25$, 0.50, and 0.75, respectively. These calculated values essentially obey the Vegard's rule. (The deviations are less than 0.4%.) The Zn-Se and Cd-Se bond

TABLE IV. The coordinates of the atoms in the cubic unit cell for $x=0.75$. The values are given in terms of the equilibrium lattice constant $\eta=0.00875$.

atoms	x	y	z
Zn	0.25	0.25	0.25
Zn	0.25	0.75	0.75
Zn	0.75	0.25	0.75
Be	0.75	0.75	0.25
Se	$-\eta$	$-\eta$	$-\eta$
Se	$-\eta$	$0.5+\eta$	$0.5+\eta$
Se	$0.5+\eta$	$-\eta$	$0.5+\eta$
Se	$0.5+\eta$	$0.5+\eta$	$-\eta$

TABLE V. Bond lengths $d_{\text{Zn-Se}}$ and $d_{\text{Cd-Se}}$, in Å in the $Zn_{1-x}Cd_xSe$ alloy.

x	$d_{\text{Zn-Se}}$	$d_{\text{Cd-Se}}$
0.00	2.480	
0.25	2.474	2.648
0.50	2.453	2.644
0.75	2.422	2.630
1.00		2.618

TABLE VI. Bond lengths $d_{\text{Zn-Se}}$ and $d_{\text{Zn-Te}}$ in the $ZnSe_{1-x}Te_x$ alloy (in Å).

x	$d_{\text{Zn-Se}}$	$d_{\text{Zn-Te}}$
0.00	2.480	
0.25	2.480	2.580
0.50	2.474	2.583
0.75	2.464	2.581
1.00		2.574

lengths obtained for $x=0.000.25$, 0.50 0.75, and 1.00 are tabulated in Table V and are plotted in Fig. 2. The coordinates of the atoms in the unit cell are the same as those shown in Tables II, III, and IV, with Be replaced by Cd and with $\eta=0.0132$, 0.0283, and 0.01486 for $x=0.25$, 0.50, and 0.75, respectively. (Though these η's are larger than those of the $Zn_{1-x}Be_xSe$ alloys, it does not necessarily mean that the bond lengths have larger deviations from those of the endpoint binaries. The η's in the $Zn_{1-x}Be_xSe$ case are smaller because the Be-Se bond length increases significantly and becomes close to the Zn-Se bond length as shown in Fig. 1.) The bond lengths $d_{\text{Zn-Se}}$ and $d_{\text{Cd-Se}}$, deviate from those of their respective Zn-Se and Cd-Se binaries within about -2 and $+1$ %, respectively. The bond-length results show that in the $A_{1-x}B_xC$-type semiconductor alloys, the cation-anion bond lengths do not deviate much from those of the respective binaries if the covalent sizes of the A and B ions themselves do not differ greatly.

Zn-Se and Cd-Se lattice constants differ by 6.5%. While Zn-Se and Zn-Te lattice constants differ by 7.4%, which is only about 1% larger. Based on the calculated lattice constants for $Zn_{1-x}Cd_xSe$ stated previously, we expect that the lattice constants of the $ZnSe_{1-x}Te_x$ alloys will approximately follow the Vegard's rule. Thus, we have used the lattice constants determined from the Vegard's rule directly for $ZnSe_{1-x}Te_x$ calculation. The good agreement between our calculated and the experimentally observed bowing of E_g^{Γ} suggests that our use of the Vegard's rule is adequate. In addition, we have identified as to be described later that the bowing of E_g^{Γ} is not due to the deviations of the cation-anion bond lengths or lattice constants but due to the significant difference in the electronegativities of Se and Te ions. We then apply the MD method to calculate the equilibrium values of the Zn-Se and Zn-Te bond lengths $d_{\text{Zn-Se}}$ and $d_{\text{Zn-Te}}$, of the $ZnSe_{1-x}Te_x$ alloy. Specifically, we carry out this calculation for $x=0.25$, 0.50, and 0.75. The calculated $d_{\text{Zn-Se}}$ and $d_{\text{Zn-Te}}$ are tabulated in Table VI. Our results show that $d_{\text{Zn-Se}}$ and $d_{\text{Zn-Te}}$ are essentially conserved in the $ZnSe_{1-x}Te_x$ alloy within 0.016 Å (or 0.6%) relative to their value in the corresponding binary compound despite that $d_{\text{Zn-Se}}$ and $d_{\text{Zn-Te}}$ differ by 7.4%.

We consider short-period sinusoidally modulated $ZnSe_{1-x}Te_x$ superlattices, since this affords us the opportunity to explore similarities and differences between such periodic systems and random alloys with the same average composition. As a representative example we have chosen a superlattice in which the composition x varies sinusoidally along the [100] direction between 0.25 and 0.75 (i.e., x av-

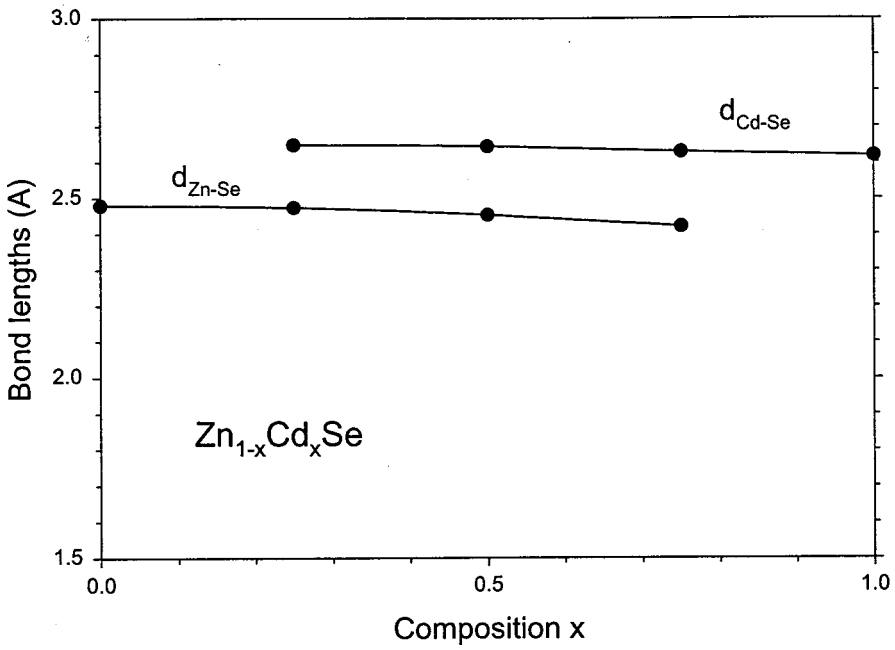

FIG. 2. Bond lengths $d_{\text{Zn-Se}}$ and $d_{\text{Cd-Se}}$, are plotted with respect to the composition x for the $Zn_{1-x}Cd_xSe$ alloy.

TABLE VII. Bond lengths $d_{\text{Zn-Se}}$ and $d_{\text{Zn-Te}}$ in the $ZnSe_{1-x}Te_x$ superlattice (in Å) for $0.25<x<0.75$. The parameter σ represents standard deviation.

x	$d_{\text{Zn-Se}}$	$d_{\text{Zn-Te}}$
0.00	2.480 (expt. 2.454)	
0.25	2.487 ($\sigma=0.026$)	2.616 ($\sigma=0.019$)
0.50	2.462 ($\sigma=0.039$)	2.596 ($\sigma=0.040$)
0.75	2.440 ($\sigma=0.030$)	2.571 ($\sigma=0.037$)
100		2.574 (expt. 2.642)

erages to 0.50). We assume a lattice parameter of 5.837 Å for this structure, i.e., we take it to be the average of Zn-Te and Zn-Se lattice constants. For performing the calculation we have chosen the cell $(a\times 2a\times 4a)$, with the z coordinate in the [001] direction. The unit cell contains eight cation-anion bilayers. Each bilayer contains four Zn ions and four Se/Te ions. Within the unit cell, the numbers of Te ions in these eight bilayers are 1, 1, 2, 2, 3, 3, 2, 2, respectively. The corresponding compositions are $\frac{1}{4}$, $\frac{1}{4}$, $\frac{1}{2}$, $\frac{1}{2}$, $\frac{3}{4}$, $\frac{3}{4}$, $\frac{1}{2}$, and $\frac{1}{2}$, respectively. Since we are limited by our calculation method, we have to choose a piecewise or stepwise variation of the composition rather than a continuous sinusoidal function. We have therefore chosen the above sequence of compositions as an approximation of the sinusoidal distribution of anions in the structure of interest.

The energy minimization calculation is carried out on this system until the force criterion for the equilibrium atomic positions stated previously is satisfied. The process reveals significant variations of $d_{\text{Zn-Se}}$ and $d_{\text{Zn-Te}}$. Calculated $d_{\text{Zn-Se}}$ and $d_{\text{Zn-Te}}$ are tabulated in Table VII. It is immediately clear that the bond lengths in the superlattice differ substantially from those of the random $ZnSe_{1-x}Te_x$ alloy. In particular, we find interesting trends in the variation of $d_{\text{Zn-Se}}$ and $d_{\text{Zn-Te}}$ with respect to x. In the $x=0.25$ region of the superlattice, where Se is the majority anion, $d_{\text{Zn-Se}}$ is very close to that of the binary compound Zn-Se, while in the $x=0.75$ region, where Te is the majority, $d_{\text{Zn-Te}}$ is very close to that of the binary compound Zn-Te. On the other hand, in the region where Se is the minority, $d_{\text{Zn-Se}}$ is significantly decreased, while in the region where Te is the minority, $d_{\text{Zn-Te}}$ is significantly increased. These trends indicate that Zn-Se and Zn-Te bonds compete in trying to conserve their binary bond lengths. In the $x=0.25$ region the majority Se atoms dominate, pulling the Zn atoms away from the Te atoms, so that $d_{\text{Zn-Te}}$ is increased by about 1.7%. And in the $x=0.75$ region, the majority Te atoms win and push the Zn atoms towards the Se atoms, so that $d_{\text{Zn-Se}}$ is decreased by a comparable amount of about 1.9%. These properties arise from the fact that constraint of the atomic arrangements in the $x=0.25$ and 0.75 regions must have the same average lattice periodicity as in the $x=0.50$ region. In contrast, in the case of the $ZnSe_{1-x}Te_x$ alloy, the Zn-Se and Zn-Te bond lengths are uniform and binarylike throughout.

IV. ELECTRONIC STRUCTURE

In calculating the electronic structure of $Zn_{1-x}Be_xSe$, we have chosen the basic cubic unit cell and sampled the four special **k** points of Chadi and Cohen[24] for a cubic lattice to obtain the self-consistent potential. The self-consistent potential is then used to calculate E_g^Γ. We have calculated E_g^Γ's for $x=0.0$, 0.25, 0.50, 0.75, and 1.0 on the same footing to avoid errors caused by the use of different unit cells and different **k** points. Although the percentage errors of the calculated equilibrium lattice constants are typical of LDA calculations, these errors are not similar or proportional for the various binaries considered, so that they will give rise to incorrect trend of E_g^Γ, since E_g^Γ is very sensitive to the deviation of the bond length. For example, the change of E_g^Γ with respect to the bond length is ~ 7 eV/Å, which will give rise to a deviation in E_g^Γ by 0.14 eV if the bond length deviates by only 0.02 Å. The direct use of the lattice constant determined from MD calculation will then defeat our purpose of looking for the physical origin of the bowing of E_g^Γ. Thus, in electronic structure calculations, we need to prorate the atomic positions obtained by MD calculations with the experimental MD lattice constant ratio.

Since to our knowledge the experimental lattice constants for these alloys are not available, we have tried to devise a reasonable way to overcome the accuracy problem stated above. We have chosen the lattice constant $a(x)$ by the equation $a(x)=a_{\text{calc}}(x)(a_{\text{Vg}}^{\text{exp}\,t}/a_{\text{Vg}}^{\text{calc}})$, where $a_{\text{Vg}}^{\text{exp}\,t}$ and $a_{\text{Vg}}^{\text{calc}}$ are the lattice constants evaluated using the Vegard's rule with the experimental and calculated end-point lattice constants, respectively, and $a_{\text{calc}}(x)$ is the equilibrium lattice constant obtained by MD calculations. We then adjust η to obtain cation-anion bond lengths that have the same ratio as that obtained by MD calculations as given in Table I. In this way, we can keep the trend of the deviations of the bond lengths close to that determined by MD calculations.

The calculated E_g^Γ's for $Zn_{1-x}Be_xSe$ are 2.265, 2.480, 2.844, 3.461, and 4.750 eV, respectively, for $x=0.00$, 0.25, 0.50, 0.75, and 1.00. The calculated E_g^Γ's and the experimental data of Peiris *et al.*[5] and of Chauvet, Tournie, and Faurie[6] are plotted in Fig. 3. E_g^Γ's are underestimated as expected. Figure 3 shows that E_g^Γ bows down. The bowing of E_g^Γ seems to reflect the elongation of the Be-Se bond as shown in Fig. 1. In the region $x\leqslant 0.5$ the average slope is 1.16 eV, which is about one half of the experimental data of 2.3 eV.[5,6] Despite the significant underestimate of the slope and the overestimate of the bowing, our calculated $E_g^\Gamma(x)$ shows a similar trend to that of the experimental data as shown in Fig. 3. That is $E_g^\Gamma(x)$ is approximately linear with a slight downward bowing in the region $x\leqslant 0.50$. This property can be attributed to the near constant values of both $d_{\text{Be-Se}}$ and $d_{\text{Zn-Se}}$ in this region as shown in Fig. 1.

Calculated E_g^Γ's for $Zn_{1-x}Cd_xSe$ are 2.265, 1.874, 1.704, 1.535, and 1.478 eV, respectively, for $x=0.00$, 0.25, 0.50, 0.75, and 1.00. Calculated E_g^Γ's and the experimental data of Peiris *et al.*[5] are plotted in Fig. 4. The dashed line shown in this figure is a straight line linking the E_g^Γ's of the Zn-Se and Cd-Se binaries. In this figure, the experimental E_g^Γ can be seen to bow down slightly. The calculated E_g^Γ also bows down. However, our calculation overestimates the bowing. For $x\leqslant 0.5$, the calculated E_g^Γ as a function of x has a slope

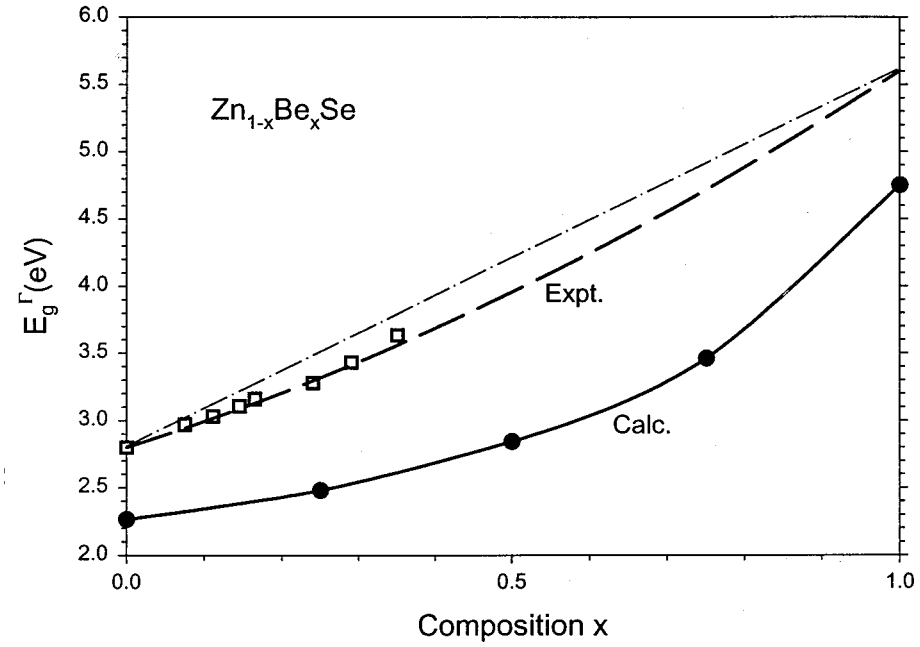

FIG. 3. E_g^Γ versus the composition x for the $Zn_{1-x}Be_xSe$ alloy. The solid circles and open squares are the calculated E_g^Γ's and the experimental E_g^Γ's of Peiris *et al.* (Ref. 2), respectively. The dashed line shows the quadratic equation fitted from the experimental data by Chauvet, Tournie, and Faurie (Ref. 3). The thin dash-dotted straight line is a guide to show the bowing of E_g^Γ.

of -1.12 eV, which is in good agreement with the experimental value of -1.20 eV. For $x>0.5$, the calculated E_g^Γ has a slope of -0.25 eV, which is much smaller in magnitude than the experimental value of -0.90 eV. The discrepancy between calculated and experimental slopes of $E_g^\Gamma(x)$ for $x>0.5$, for which the Cd ion is the majority cation, may be due to a deficiency in LDA, which gives rise to a smaller error in the E_g^Γ for Cd-Se than for Zn-Se.

The calculated values of E_g^Γ for $ZnSe_{1-x}Te_x$ for $x=0.00$, 0.25, 0.50, 0.75, and 1.00 are 2.265, 1.899, 1.663, 1.616, and 1.754 eV, respectively. These are plotted in Fig. 5. The difference between the calculated E_g^Γ for Zn-Se and Zn-Te is 0.511 eV, which is somewhat larger than the experimental values of 0.32 eV at room temperature[23] and 0.43 eV at 4 K.[1] Figure 5 shows that E_g^Γ as a function of x bows down with a minimum of 1.61 eV at about $x=0.67$, which is in good agreement with experimental data, where the minimum is observed at $x=0.65$.[1] The calculated bowing coefficient, i.e., the coefficient of the quadratic term, is 1.576, which again agrees quite well with the experimental value 1.621.[1] The values of E_g^Γ depend of course on the cation-anion bond length, the variation $\partial E_g^\Gamma/\partial d_{\text{Zn-Se}}$ and $\partial E_g^\Gamma/\partial d_{\text{Zn-Te}}$ being calculated to be -7.11 and -7.22 eV/Å, respectively. However, with these rates of change of E_g^Γ, the variation of the bond

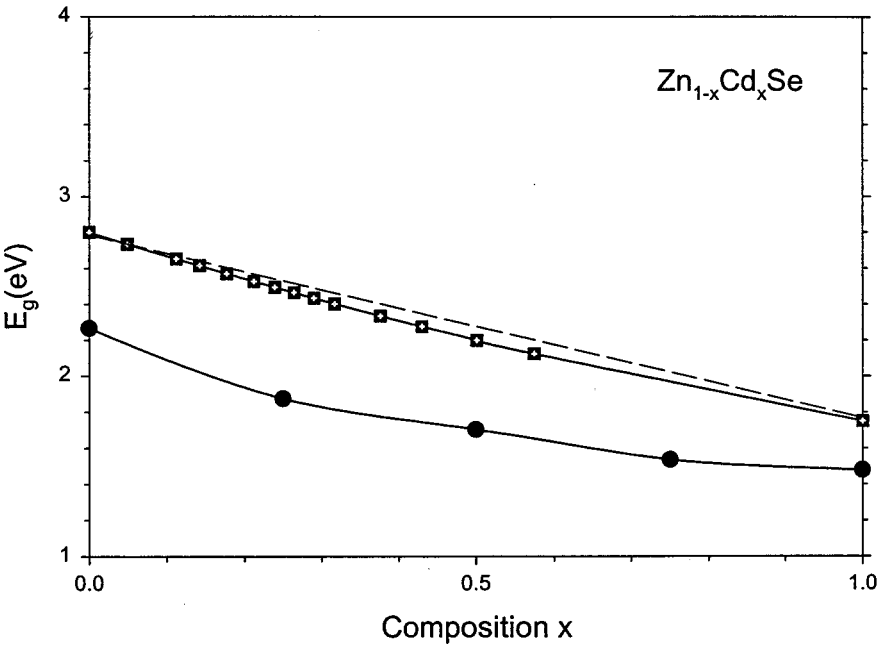

FIG. 4. E_g^Γ versus the composition x for the $Zn_{1-x}Cd_xSe$ alloy. The solid circles and open squares are the calculated and experimental E_g^Γ's, respectively.

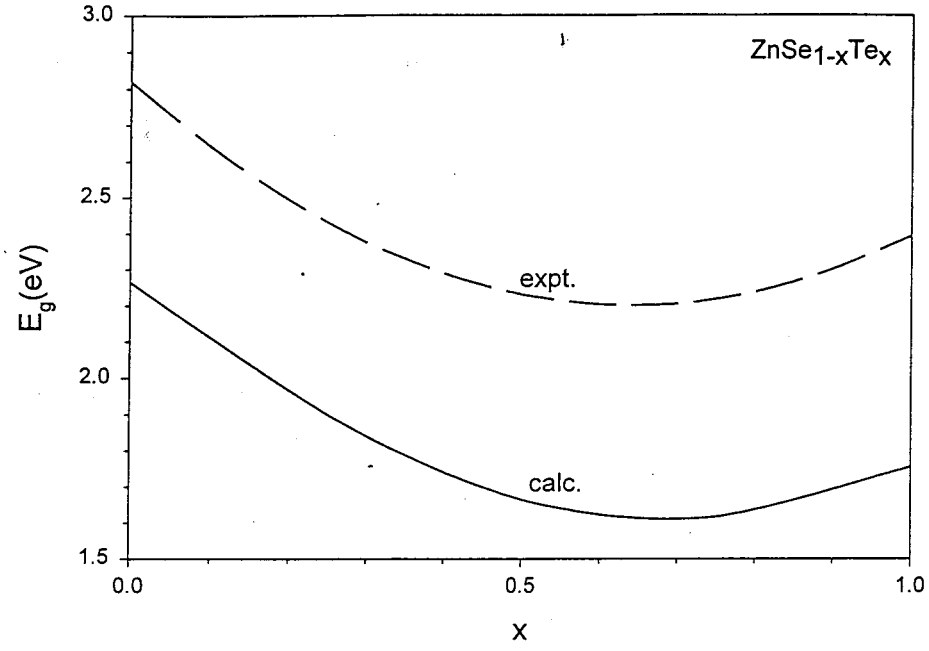

FIG. 5. Dependence of the energy gap E_g^{Γ} on composition x for $ZnSe_{1-x}Te_x$ alloys.

lengths shown in Fig. 6 cannot by itself account for the bowing of E_g^{Γ} in the $ZnSe_{1-x}Te_x$ alloy.

One must therefore look for other mechanisms that lead to bowing of E_g^{Γ}. In considering alloys of the type $AB_{1-x}C_x$ the value of E_g^{Γ} is expected to vary linearly with x only when the electronic properties of the constituents B and C (in our case, the two anions) remain approximately the same in the alloy as in the end-point binaries. In such cases the electronic states as well as E_g^{Γ} are linear averages of their respective values in the two binaries. This is not the case in the $ZnSe_{1-x}Te_x$ alloy because Se has a significantly larger electronegativity than Te (2.55 vs 2.1[4]), and there will thus occur significant charge transfer from Te to Se as mixing of the material takes place. The charge transfer from Te to Se renders the Te ions in the alloy to have a smaller negative effective charge than the Te ions in Zn-Te, and the Se ions to have a larger negative effective charge in the alloy than the Se ions in Zn-Se. Then the corresponding changes in the local Coulomb potentials are expected to render the orbital energies of the Te ions to become lower, and those of the Se ions to become higher relative to the respective binary compounds. Thus, the contributions of Te and Se ions to the state at the valence band maximum (VBM) are increased and decreased, respectively. The increased importance of the Te

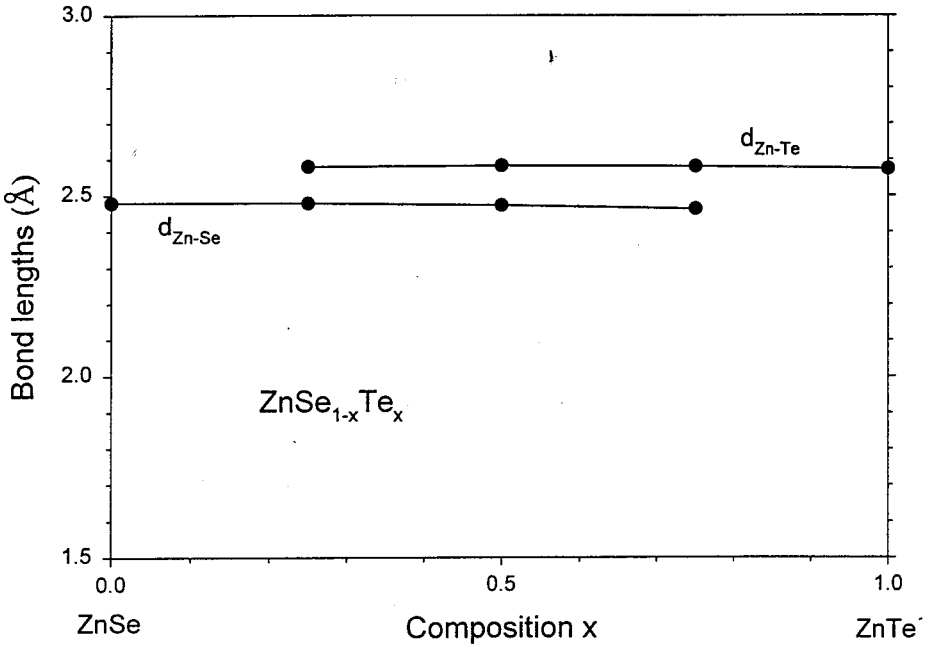

FIG. 6. The calculated bond lengths $d_{Zn\text{-}Se}$ and $d_{Zn\text{-}Te}$ as a function of the composition x for $ZnSe_{1-x}Te_x$ alloys.

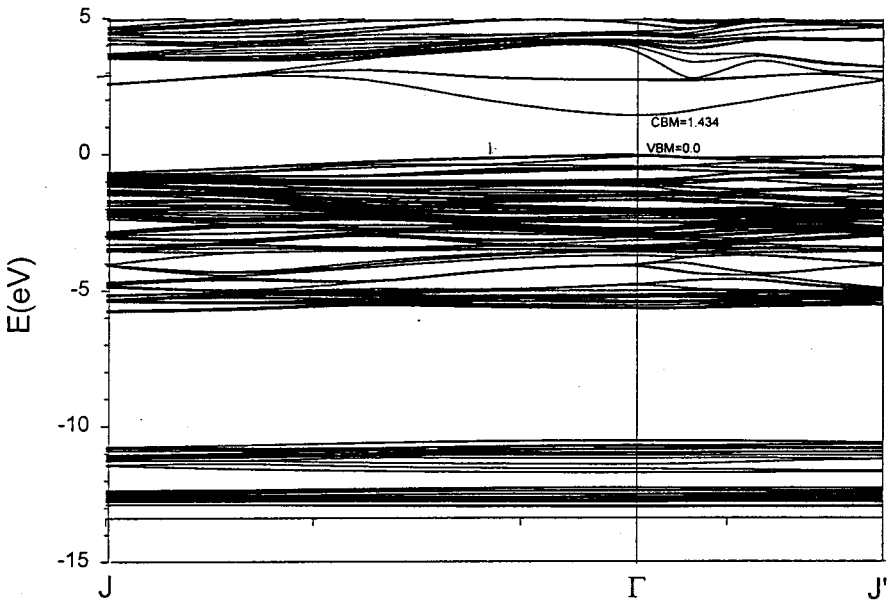

FIG. 7. Energy bands calculated for sinusoidally modulated $ZnSe_{1-x}Te_x$ short-period superlattices.

contribution means that E_g^Γ will shift towards that of ZnTe. Our calculated coefficients of the eigenvector of the state at VBM obtained for a $ZnSe_{1-x}Te_x$ alloy($x=0.50$) are 1.551 and 0.886 for Te and Se, respectively. The contribution of Te (which is proportional to the square of these coefficients) is therefore about three times larger than that of Se, consistent with the above argument.

Another effect of the charge transfer occurring in the alloy is on the conduction band. The itinerant conduction electrons are expected to shift from the neighborhood of Se ions to the neighborhood of the Te ions, since these have a reduced negative effective charge due to the charge transfer from Te to Se, and consequently their local Coulomb potential is shifted to lower their energies. Thus, the conduction band minimum (CBM) is reduced further. A combination of the two effects stated above renders E_g^Γ even lower than that of Zn-Te.

In the calculation of the electronic structure of the $ZnSe_{1-x}Te_x$ superlattice, we use the equilibrium atomic positions obtained in the MD calculations just discussed, using the experimental lattice constants. Due to the complexity of this system, we sample only one special **k** point $(2\pi/a)\times(\frac{1}{4},\frac{1}{8},\frac{1}{16})$ (Ref. 25) for the $(a,2a,4a)$ unit cell to obtain the self-consistent potential, which is then used to calculate the electronic structure. The energy bands are shown in Fig. 7 from J, $(2\pi/a)(1/2,0,0)$, to Γ and from Γ to J', $(2\pi/a)\times(0,1/4,0)$. The calculated E_g^Γ is 1.43 eV, which is smaller than the minimum calculated E_g^Γ of the $ZnSe_{1-x}Te_x$ alloy by 0.18 eV. The redshift in E_g^Γ is comparable to the 0.14 eV dispersion of the PL peak towards a lower value of 2.08 eV observed by Yang *et al.*[2] and Lee *et al.*[3] From the occupations of the anion orbitals in the $x=0.25$, 0.50, and 0.75 regions for the states in the vicinity of VBM, we find that there is no VBM offset between $x=0.50$ and 0.75 regions of the superlattice, but there is a -0.064 eV offset in the $x=0.25$ region relative to that in the $x=0.50$ (or the 0.75) region. Due to the itinerant nature of conduction electrons CBM has negligible offset among the three regions. The VBM offset results reflect the trend of variation of E_g^Γ shown in Fig. 1, though the magnitude of the variation is greatly reduced in the superlattice. The above reduction in the VBM offset can be attributed to the small layer thickness characteristic of these short-period superlattices, as well as to the absence of well-defined interfaces due to the sinusoidal (i.e., smooth) modulation of the composition. The period of our structural model is 23.54 Å, which is representative of the 13.5 to 58 Å range of the $ZnSe_{1-x}Te_x$ superlattice samples used in the PL measurements of Yang *et al.*[2] and Lee *et al.*[3]

V. CONCLUSION

We have employed the real-space density-functional molecular-dynamics and conventional electronic-structure calculation methods to study electronic and structural properties of $Zn_{1-x}Be_xSe$, $Zn_{1-x}Cd_xSe$, and $ZnSe_{1-x}Te_x$ alloys and $ZnSe_{1-x}Te_x$ superlattices. For $ZnSe_{1-x}Te_x$ we have focused on understanding the pronounced bowing phenomenon of E_g^Γ in alloys and the redshift of E_g^Γ in superlattices. The bowing of E_g^Γ is found to be attributable to significant electronegativity difference between the two aions. The calculated E_g^Γ's have a minimum at $x=0.67$ in good agreement with experimental data. The calculation for the structure of sinusoidally modulated $ZnSe_{1-x}Te_x$ superlattices whose composition varies in the range of $0.25<x<0.75$ yields an elongation of the Zn-Te bond and a contraction of the Zn-Se bond relative to those of the corresponding binary compounds. The elongation of the Zn-Te bond may explain the redshifts of E_g^Γ of 0.14 eV observed in the photoluminescence measurements on these supperlattices.

For $Zn_{1-x}Be_xSe$ and $Zn_{1-x}Cd_xSe$ we have focused on understanding bond length conservation in these alloys. We are particularly interested in whether Zn-Se and Be-Se bond

lengths are conserved in $Zn_{1-x}Be_xSe$ because Zn and Be have very different covalent radii. We find that in the $Zn_{1-x}Be_xSe$ alloys the Zn-Se bond length decreases slightly by 2.2%, while the Be-Se bond length increases by 10% relative to those of the binary compounds. This result suggests a softening of the Be-Se bond in the $Zn_{1-x}Be_xSe$ alloys. For $Zn_{1-x}Cd_xSe$, the Zn-Se and Cd-Se bond lengths deviate from those of the respective binary compounds by not more than 2% because the covalent radii of Zn and Cd do not differ excessively. We also find that the direct band gap E_g^{Γ} as a function of x bows down for both $Zn_{1-x}Be_xSe$ and $Zn_{1-x}Cd_xSe$ in agreement with experimental data, though we overestimate the bowing.

ACKNOWLEDGMENTS

M.-H. Tsai is grateful to the National Science Council of R.O.C. for their financial support (Grant No. 37127F). The work at Notre Dame was supported by the U.S. Department of Energy Grant No. 97ER45644.

[1] M. J. S. P. Brasil, R. E. Nahory, F. S. Turco-Sandroff, H. L. Gilchrist, and R. J. Martin, Appl. Phys. Lett. **58**, 2509 (1991).
[2] G. Yang, S. Lee, and J. K. Furdyna, Phys. Rev. B **61**, 10 978 (2000).
[3] S. Lee, U. Bindley, J. K. Furdyna, P. M. Reimer, and J. R. Buschert, J. Vac. Sci. Technol. B **18**, 1518 (2000).
[4] *Table of Periodic Properties of the Elements* (Sargent-Welch Scientific Company, Illinois, 1980).
[5] F. C. Peiris, S. Lee, U. Bindley, and J. K. Furdyna, J. Appl. Phys. **86**, 719 (1999).
[6] C. Chauvet, E. Tournie, and J.-P. Faurie, Phys. Rev. B **61**, 5332 (2000).
[7] O. F. Sankey and D. J. Niklewski, Phys. Rev. B **40**, 3979 (1989).
[8] M.-H. Tsai, O. F. Sankey, and J. D. Dow, Phys. Rev. B **46**, 10 464 (1992).
[9] M.-H. Tsai and K. C. Hass, Phys. Rev. B **52**, 16 420 (1995).
[10] R. V. Kasowski, M.-H. Tsai, T. N. Rhodin, and D. D. Chambliss, Phys. Rev. B **34**, 2656 (1986).
[11] D. R. Hamann, M. Schlüter, and C. Chiang, Phys. Rev. Lett. **43**, 1494 (1979).
[12] G. B. Bachelet, D. R. Hamann, and M. Schlüter, Phys. Rev. B **26**, 4199 (1982).
[13] D. M. Ceperley and G. J. Alder, Phys. Rev. Lett. **45**, 566 (1980).
[14] M.-H. Tsai, C. F. Liu, and L.-K. Hsu, Phys. Rev. B **58**, 6764 (1998).
[15] C.-M. Lin, M.-H. Tsai, T. J. Yang, and D. S. Chuu, Phys. Rev. B **56**, 9209 (1997).
[16] M.-H. Tsai, C. F. Liu, and C. S. Chang, Phys. Rev. B **54**, 7637 (1996).
[17] M.-H. Tsai, W.-M. Hu, J. D. Dow, and O. F. Sankey, J. Vac. Sci. Technol. A **10**, 2511 (1992).
[18] M.-H. Tsai, J. C. Jiang, and S. H. Lin, Phys. Rev. B **54**, R11 141 (1996).
[19] M.-H. Tsai, J. C. Jiang, and S. H. Lin, Phys. Rev. B **56**, 12 127 (1997).
[20] O. K. Andersen, Phys. Rev. B **12**, 3060 (1976).
[21] L. Hedin and B. I. Lundqvist, J. Phys. C **4**, 2064 (1971).
[22] D. A. Müller, D. J. Singh, and J. Silcox, Phys. Rev. B **57**, 8181 (1998).
[23] *CRC Handbook of Chemistry and Physics*, 73rd ed., edited by David R. Lide (CRC, Boca Raton, 1992).
[24] D. J. Chadi and M. L. Cohen, Phys. Rev. B **8**, 5747 (1973).
[25] H. J. Monkhorst and J. D. Pack, Phys. Rev. B **13**, 5188 (1976).